Published in final edited form as:
J Am Coll Cardiol. 2011 February 22; 57(8): 891–903. doi:10.1016/j.jacc.2010.11.013.

Assessment of Myocardial Fibrosis with Cardiac Magnetic Resonance

Mewton Nathan, MD PhD[1,2], **Liu Chia Ying, PhD**[1], **Croisille Pierre, MD PhD**[2], **Bluemke David, MD PhD**[1,3], and **Lima João, AC, MD MBA**[1]

[1]Johns Hopkins University, Division of Cardiology, Baltimore, MD, USA

[2]Hôpital Cardiovasculaire Louis Pradel, Departement de Radiologie, Hospices Civils de Lyon, Lyon, FRANCE

[3]Radiology and Imaging Sciences, National Institutes of Health Clinical Center, National Institute of Biomedical Imaging and Bioengineering, Bethesda, MD, USA

Abstract

Diffuse interstitial or replacement myocardial fibrosis are common features of a broad variety of cardiomyopathies. Myocardial fibrosis leads to impaired cardiac diastolic and systolic function and is related to adverse cardiovascular events. Cardiac magnetic resonance (CMR) may uniquely characterize the extent of replacement fibrosis and may have prognostic value in various cardiomyopathies. Myocardial T_1 mapping is an emerging technique that could improve CMR's diagnostic accuracy especially for interstitial diffuse myocardial fibrosis. As such, CMR could be integrated in the monitoring and the therapeutic management of a large number of patients. This review summarizes the advantages and limitations of CMR for the assessment of myocardial fibrosis.

Introduction

One of the most common histologic features of the failing heart is myocardial fibrosis. Replacement fibrosis, often present in the terminal stages of heart failure, has been reported in histopathological autopsy studies (1, 2). The pathophysiological mechanisms that lead to this fibrosis are various, some being acute as in myocardial infarction (3), others being progressive and potentially reversible as in hypertensive cardiomyopathy (4). Myocardial fibrosis in animals and patient studies is associated with worsening ventricular systolic function, abnormal cardiac remodeling, and increased ventricular stiffness (5–7). In recent clinical studies fibrosis has also been shown to be a major independent predictive factor of adverse cardiac outcome (8–12).

In the therapeutic guidelines for heart failure due to various cardiomyopathies, there are no specific therapeutic strategies based on the tissue composition of the myocardial wall either in the early or more advanced stages of disease. This lack of specific treatment might lead to

Corresponding Author: João A. C. Lima, M.D., MBA, Professor of Medicine and Radiology, Director of Cardiovascular Imaging, Johns Hopkins University, Division of Cardiology, Department of Medicine, 600 N. Wolfe Street/Blalock 524, Baltimore, Maryland 21287-0409, Phone: (410) 614-1284/FAX (410) 614-8222, jlima@jhmi.edu.

inappropriate therapies leading to increased morbidity and additional financial burden to health care services (13). Lack of personalized treatment is also secondary to the absence of accurate clinical tools to precisely phenotype patients with heart disease.

Recent reports have demonstrated the advantages of using cardiovascular magnetic resonance (CMR) for the non-invasive imaging of heart failure patients (14, 15). CMR has been established as the reference imaging method for the assessment of cardiac anatomy and function by providing highly accurate and reproducible measures of both the left and right ventricles and also for the assessment of myocardial viability (16–18). The field of CMR is rapidly evolving with continuing technologic progress and the recent development of applications that have further enhanced its capacity to characterize myocardial tissue. In this review we will focus on the CMR characterization of the different types of myocardial fibrosis and its etiology through late gadolinium enhancement and T_1 mapping.

Myocardial Fibrosis: Pathogenesis and Consequences

Fibrosis Pathophysiology

In physiological conditions, the fibrillar collagen network is in intimate contact with all the different cell-types of the myocardium and plays a critical role in the maintenance of ventricular shape, size and function (Figure 1).

Myocardial fibrosis defined by a significant increase in the collagen volume fraction (CVF) of myocardial tissue is always present in end-stage heart failure (19). The distribution of myocardial fibrosis however is variable according to the underlying pathology and accounts for discrepancies among different pathological reports where only qualitative as opposed to quantitative measurements were made (19–22). The progressive accumulation of collagen accounts for a spectrum of ventricular dysfunctional processes that commonly affect diastole first, and subsequently involve systolic performance (5).

Subtypes of Myocardial Fibrosis

Different types of myocardial fibrosis have been reported according to the cardiomyopathic process (Figure 1).

Reactive Interstitial Fibrosis—The first type of fibrosis is interstitial reactive fibrosis with a diffuse distribution within the interstitium but which can also be more specifically perivascular (23). This type of fibrosis has a progressive onset and follows the increase in collagen synthesis by myofibroblasts under the influence of different stimuli. It has mostly been described in hypertension and diabetes mellitus where the activation of the renin-angiotensin aldosterone system, β-adrenergic system, the excess of reactive oxygen species and metabolic disturbances induced by hyperglycemia are major contributors (23–27) (Figure 2). But this type of fibrosis is also present in the aging heart, in idiopathic dilated cardiomyopathy (2, 21) and in left ventricular pressure-overload and volume-overload states induced by chronic aortic valve regurgitation and stenosis (28, 29). It has also been reported in the remote non-infarcted myocardium after infarction (30).

Interstitial fibrosis is an intermediate marker of disease severity, as it has been shown in hypertensive cardiomyopathy, and it precedes irreversible replacement fibrosis (27, 31). It is reversible under specific therapy (4, 32, 33). Therefore there is some clinical interest in its assessment for the management of patients with hypertension, diabetes, primary dilated cardiomyopathy and valvular disease.

Infiltrative Interstitial Fibrosis—This subtype of fibrosis is induced by the progressive deposit of insoluble proteins (amyloidosis) or glycosphingolipids (Anderson Fabry's

disease) (34, 35) in the cardiac interstitium. Although this subject is not the primary focus of this review, their pathophysiology follows similar patterns and the early detection of cardiac involvement is of critical importance to therapeutic management.

Replacement Fibrosis—This replacement or scarring fibrosis corresponds to the replacement of myocytes after cell damage or necrosis by plexiform fibrosis, mainly type I collagen (36). Replacement fibrosis appears as soon as the myocyte integrity is affected. It can have a localized distribution (ischemic cardiomyopathy, myocarditis, hypertrophic cardiomyopathy, sarcoidosis) or a diffuse distribution (chronic renal insufficiency, toxic cardiomyopathies, miscellanous inflammatory disease) according to the underlying etiology (14, 15, 37). Interstitial fibrosis and infiltrative fibrosis ultimately lead to replacement fibrosis in the later stages of disease where cellular damage and cardiomyocyte necrosis/apoptosis appear (27).

Detection of Myocardial Fibrosis

Endomyocardial Biopsies

Previously, the only methodology available to assess myocardial fibrosis was the histopathology assessment of endomyocardial tissue biopsies or of autopsy pieces. This methodology enables qualitative macroscopic assessment after Masson's Trichrome staining (22) and quantitative absolute assessment of the CVF in tissue samples by quantitative morphometry with picrosirius red that specifically stains fibrillar collagen under polarized light (1, 21, 38). Although this technique offers an absolute quantification of fibrosis in myocardial samples (3) it has three evident drawbacks: 1) invasive biopsies are required; 2) sampling error restricts the accuracy of biopsy in the case of localized fibrosis (7, 39); 3) fibrotic involvement of the whole left ventricle cannot be determined.

Cardiac Magnetic Resonance

In the last 10 years, CMR has emerged as a non-invasive imaging method that allows a comprehensive assessment of myocardial anatomy and function with unequaled levels of accuracy and reproducibility. The use of gadolinium extracellular contrast agents with CMR using late postgadolinium myocardial enhancement sequences (LGE) have further pushed our ability to accurately and precisely analyze myocardial tissue composition, especially myocardial fibrosis content.

Physical Basis of CMR Tissue Characterization

T_1, T_2 relaxation times, proton density: In CMR images, the pixel signal intensity is based on the relaxation of hydrogen nuclei protons in the static magnetic field, of typically 1.5 or 3.0-Tesla scanners. The relaxation of the hydrogen nucleus proton is specifically characterized by 2 distinct MR relaxation parameters: 1) the longitudinal relaxation time (T_1) or spin-lattice relaxation time that corresponds to the specific time decay constant when the proton recovers approximately 63% of its longitudinal magnetization equilibrium value; 2) the transverse relaxation time (T_2) or spin-spin relaxation time that corresponds to the specific time when the proton transverse magnetization drops to approximately 37% of its original value. Both of those times are measured in milliseconds. Another constitutional parameter that needs to be added to explain the pixel signal intensity is the density of mobile hydrogen atoms within the tissue voxel or proton density.

Both the T_1 and T_2 relaxation times depend on the molecular environment of the water molecules in the tissue and therefore characterize each tissue very specifically. T_1 and T_2 relaxation times vary significantly from one type of tissue to another, but also within the same tissue depending on its physiopathological status (inflammation, edema, fibrosis). The

CMR imaging techniques used will also result in different contrast images. Specific CMR sequences can be used to selectively reveal certain molecular environments within the tissue. Those differences are further enhanced with the use of gadolinium extracellular magnetic resonance contrast agents.

Gadolinium CMR Enhancement: Gadolinium contrast agents reduce the T_1 relaxation time of adjacent tissue. Thus the local gadolinium tissue concentration will induce differences in signal intensity in the T_1-weighted image. Based upon various specific properties of the tissue the T_1 shortening induced by the gadolinium contrast agent will generate specific differences in signal intensity. The major tissue parameters that will influence the final voxel signal intensity in the contrast-enhanced images are: local perfusion, extracellular volume of distribution, water exchange rates among the vascular, interstitial and cellular spaces and wash-in and wash-out kinetics of the contrast agent (40, 41).

Gadolinium Enhanced CMR of Myocardial Fibrosis: The physiological basis of the LGE of myocardial fibrosis is based upon the combination of an increased volume of distribution for the contrast agent and a prolonged washout related to the decreased capillary density within the myocardial fibrotic tissue (40, 42). The increase in gadolinium concentration within fibrotic tissue causes T_1 shortening which appears as bright signal intensity in the CMR image based on conventional inversion-recovery gradient echo sequences. Thus the discrimination between scarred/fibrotic myocardium and normal myocardium relies on contrast concentration differences combined with the chosen setting of the inversion-recovery sequence parameters. These parameters are set to “null” the normal myocardial signal that will appear dark in the final image relative to the bright signal of the scarred/fibrotic myocardium.

Of note, gadolinium contrast agents are not specific markers for myocardial fibrosis. Late gadolinium enhancement is caused by modifications of the contrast distribution space as well as wash-in and out kinetics of the contrast into interstitial space or extra-cellular matrix. Therefore, quantification of late enhancement (e.g., T_1 mapping) explores the volume of the extra-cellular matrix. This volume is increased in myocardial fibrosis but can also be increased in other pathological processes, such as inflammation and edema.

Measuring Myocardial Fibrosis with Late Gadolinium Enhancement

Clinical Applications: The clinical application of myocardial LGE with CMR started with the assessment of experimental acute myocardial infarction followed by measurements in chronic infarct experimental models and patients (43–45). After having shown that the regional differences in signal intensity were correlated to the extent and severity of myocardial injury, Kim et al. reported in experimental studies that the spatial extent of hyperenhancement was the same as the spatial extent of the collagenous scar at 8 weeks with highly significant correlations (46). The clinical impact of LGE extent in patients with chronic ischemic cardiomyopathy was further demonstrated with the clinical study in 50 patients undergoing revascularization showing that the degree of improvement in the global mean wall-motion score and the ejection fraction was significantly related to the transmural extent of LGE (45).

During the chronic phase of infarction, when a dense fibrotic scar replaces the infarcted myocardium, Mahrholdt et al. showed the accuracy and the clinical reproducibility of delayed enhancement for infarct size determination (17). Moreover Wu et al. showed the higher sensitivity for infarct detection by LGE-CMR compared to SPECT, and other studies have confirmed the ability of CMR to detect microinfarctions (47, 48).

The number of studies assessing myocardial fibrosis by LGE in other types of cardiomyopathies has dramatically increased in the last ten years (Table 1). Different patterns of enhancement have been reported according to the underlying etiology and LGE CMR has become a first-line non-invasive exam for the etiologic assessment of new onset myocardial dysfunction (14, 15, 49).

LGE-CMR also provides prognostic information that could be used to define more appropriate therapeutic strategies. In ischemic cardiomyopathy, the transmural extent of LGE is predictive of myocardial wall recovery after revascularization, but it is also predictive of adverse LV remodeling (45, 50). At the clinical level, infarct size is an independent prognostic factor for heart failure, arrhythmic events and cardiac mortality (9, 11, 51). In non-ischemic dilated cardiomyopathy, Assomull et al. showed that the presence of myocardial LGE was associated with a 3-fold increase of hospitalization for heart failure or cardiac death and a 5-fold increase of sudden cardiac death or ventricular arrhythmias (8). In hypertrophied cardiomyopathy (HCM), Rubinshtein et al reported that LGE was strongly associated with arrhythmia and remained significantly associated with subsequent SCD after adjustment for other risk factors (52, 53). In the same way, LGE is significantly and independently associated with adverse cardiac events in patients with cardiac amyloidosis (54) and in patients undergoing aortic valve replacement (55). Recently, the additional prognostic value of LGE was demonstrated in hypertensive (56) and diabetic (12) patients free of any cardiac symptoms and with preserved ejection fraction. Finally, the clinical significance of LGE also offers potential targets for new therapeutic strategies designed for the purpose of personalizing medical management, although such paradigm requires further development and testing. In this regard, there is a crucial need for LGE-CMR assessment's standardization in clinical practice (57).

LGE Limitations: If LGE allows a sensitive and reproducible qualitative assessment of myocardial replacement fibrosis, it is limited in its accuracy for absolute quantification of myocardial fibrosis and the assessment of diffuse fibrosis is restricted by technical and physiopathological characteristics. First, with conventional LGE imaging sequences, signal intensity is expressed on an arbitrary scale that differs from one imaging study to another and therefore is unsuitable for direct signal quantification in cross sectional or longitudinal comparisons. The late gadolinium enhanced myocardial fibrotic tissue is defined on the basis of the difference in signal intensity between fibrotic and normal myocardium and this difference generates the image contrast. In addition, LGE is influenced not only by technical parameters set during image acquisition (inversion time (58), slice thickness...) but also according to the intensity threshold that is arbitrarily set during post-processing to differentiate normal from fibrotic myocardium (59).

Presently, there is no clear consensus on the intensity threshold settings to use for clinical assessment of myocardial fibrosis. Various methods have been reported to define late enhanced myocardium, with significantly different results (59–62). This is one of the factors explaining the variability in the frequency of myocardial fibrosis found by LGE in various cardiomyopahties from different studies (Table 1). This questions the reliability and reproducibility of LGE for myocardial fibrosis quantification in a clinical setting.

Another concern with the use of myocardial LGE has emerged with its increasing use to define the myocardial "gray zone" in clinical studies. The "gray zone" has been arbitrarily defined on late enhancement CMR images as myocardium with intermediate signal intensity enhancement between normal and scarred/fibrotic myocardium (63). This area reflects tissue heterogeneity within the infarct periphery and has been shown to strongly correlate with ventricular arrythmia inducibility and post-myocardial infarction mortality in ischemic cardiomyopathy (63, 64). The use of this "gray zone" in ischemic cardiomyopathy and other

types of cardiomyopathies further expands the assessment and the quantification of hyperenhanced myocardium for purposes that go beyond pure quantification of myocardial fibrosis.

Finally, while LGE CMR is the most accurate method to measure myocardial replacement fibrosis, its sensitivity is limited for the assessment of diffuse interstitial fibrosis. In LGE CMR, image contrast relies on the difference in signal intensity between fibrotic and "normal" myocardium, and such differences may not exist if the process is diffuse.

Measuring Myocardial Fibrosis with T_1 mapping

T_1 Mapping Basics: The recent technical improvements in acquisition sequences now enable us to perform myocardial T_1 mapping with high spatial resolution by using 1.5-T MR imaging scanners within a single breath hold (65). Compared to LGE images, T_1-mapping CMR techniques allow us to eliminate the influences of windowing and variations in signal enhancement by directly measuring the underlying T_1 relaxation times. Therefore, it allows signal quantification (in milliseconds) on a standardized scale of each myocardial voxel to characterize myocardial tissue.

T_1 Mapping Methodology: A T_1 map of the myocardium is a parametric reconstructed image, where each pixel's intensity directly corresponds to the T_1 relaxation time of the corresponding myocardial voxel. Signal recovery from each myocardial voxel is sampled with multiple measurements after a specific preparation pulse sequence and the associated T_1 relaxation time is calculated from these measurements by the combination of all acquisitions. T_1 maps can be obtained anytime before or after gadolinium contrast administration. The pre-contrast T_1 map is a baseline reference. The post-contrast T_1 maps are assessed at different time points after contrast administration and could be used to obtain the curve of myocardial T_1 recovery reflecting the contrast agent washout (Figure 3).

Different CMR acquisition sequences have been used to obtain myocardial T_1 maps (6, 65–68). This is an essential point to consider before performing myocardial T_1 maps, because it directly influences the accuracy and reproducibility of the final T_1 measurements. This should also be considered when comparing results between different studies. Different T_1 mapping strategies will have varying sensitivities to, motion artifacts, heart rate and intrinsic T_1 value ranges (67).

The most assessed T_1 mapping sequence has been described by Messroghli et al. and is the MOdified Look-Locker Inversion-recovery (MOLLI) sequence (65, 67, 69–71). MOLLI provides high-resolution T_1 maps of human myocardium in native and post-contrast situations within a single breath-hold.

This sequence has been thoroughly described, optimized and tested on phantoms, healthy volunteers and ischemic cardiomyopathy patients. Even though it is sensitive to heart rate extreme values and tends to slightly underestimate the true heart T_1 value, the method allows a rapid and highly reproducible T_1 map of the heart with high levels of intra and inter-observer agreement (70). However, in the only report on the clinical validation of T_1 mapping against histology for the assessment of myocardial fibrosis, Iles et al. used a different type of sequence (VAST inversion-recovery prepared 2D fast gradient echo sequence with variable sampling of k-space) (6). This sequence, very similar to the MOLLI sequence, has less well been validated in the literature.

T_1 maps can be obtained at different slice levels with an average acquisition time of 15 to 20 seconds (one breathhold) for one T_1 map (70). Figure 4 demonstrates T_1 maps at the mid-ventricle level.

The advantages of T_1 mapping: T_1 mapping enables direct myocardial signal quantification (in milliseconds) on a standardized scale. This allows a better characterization of myocardial tissue composition on a global or regional level. Myocardial areas of delayed enhancement can be measured in terms of their spatial extent, but also in terms of the magnitude of their signal intensity: the composition of each myocardial slice can be analyzed as a T_1 distribution histogram which gives a more accurate description of the myocardial tissue composition (Figure 5). One hypothesis would be to use this T_1 distribution (mean T_1 peak value, distribution scatter) to identify specific myocardial patterns such as myocardial diffuse fibrosis, specific myopathies or the peri-infarction or "gray zone".

Pre-contrast mean T_1 value of normal myocardium is of 977±63 ms and the post-contrast values between 10 and 15 minutes of normal myocardium have been reported around 483±20 ms (70) at 1.5T. Pre-contrast T_1 values of myocardial fibrosis (infarct scar) are significantly longer than those of normal myocardium (1060±61 versus 987±34 ms) although the range of pre-contrast T_1 value distribution overlaps with that of fibrotic myocardium (71).

Post-contrast T_1 values of scarred myocardium (replacement fibrosis) are significantly shorter than those of normal myocardium due to the retention of gadolinium contrast in fibrotic tissue. Messroghli et al. reported T_1 values around 390±20 ms in chronic infarct scar compared to 483±23 ms in normal myocardium for T_1 maps obtained between 10 and 15 minutes after contrast administration at 0.15 mmol/kg (71).

The accuracy of post-contrast T_1 mapping to assess myocardial interstitial and replacement fibrosis has had limited validation. In one study of 9 patients post cardiac transplantation, T_1 time at 15 minutes post gadolinium administration showed an inverse correlation with myocardial collagen content.

Even if there is overlap between T_1 values for interstitial and replacement fibrosis, T_1 mapping can accurately differentiate both interstitial and replacement fibrosis from normal myocardium (72). In an in vitro magnetic resonance study of selected human myocardium samples, Kehr et al. showed that post-contrast T_1 values for both diffuse and replacement fibrosis were significantly different from T_1 value for normal myocardium. Although there was no significant difference between the respective diffuse fibrosis and replacement fibrosis T_1 values, there was a significant correlation between T_1 value and myocardial collagen content. Yet, the real clinical benefit of T_1 mapping remains to be shown. When applied with rigorous methodology, T_1 mapping could be the ideal tool to assess and quantify diffuse myocardial fibrosis. It could also improve the accuracy of delayed enhancement and myocardial scar characterization.

Reported Clinical Applications of T_1 Mapping: There are very few studies published using T_1 mapping in the clinical setting. They are reported in Table 2.

T_1 Mapping Limitations: To date, all of the published clinical studies using T_1 mapping have been realized on small groups of selected patients, with different types of T_1 acquisition sequences. Although the use of T_1 mapping for myocardial fibrosis assessment appears to be promising when combined with LGE imaging, its accuracy is sensitive to many confounding factors. Those factors are:

1. The physical properties of Gadolinium contrast agents (dose, concentration, relaxivity, rate of injection and water exchange rate) significantly affect the final myocardial voxel T_1 value.

2. The time delay of the T_1 mapping measurement after gadolinium administration also significantly affects the resulting T_1 values. Since the T_1 value exponentially increases with the washout of gadolinium contrast from the myocardium, the time of T_1 mapping acquisition will have a significant influence on the final myocardial voxel T_1 value (70). Therefore, in clinical studies, when performing T_1 mapping acquisition, the acquisition time after contrast administration should be carefully monitored and reported. Solutions to this problem may include normalization to noncardiac tissue (e.g., muscle, blood) or characterization of the time as a T_1 curve.
3. The types of T_1 mapping acquisition sequence that will affect the sensitivity to motion artifacts (arrythmia), heart rate and T_1 extreme values (65, 67). Recently, various acquisition protocols with shorter acquisition times have been reported with good levels of accuracy (73, 74).
4. The gadolinium myocardial washout rate which mainly depends on each patient's individual glomerular filtration rate should be carefully accounted for, when performing T_1 mapping. While the influence of renal dysfunction on myocardial T_1 mapping remains incompletely understood, Maceira et al. proposed a correction model of myocardial T_1 value by blood T_1 value in their study of cardiac amyloid patients (66) that significantly improved T_1 mapping sensitivity.
5. The presence of LGE areas will have to be accounted for in order to assess the true T_1 value of non-affected myocardial areas. Those areas have been shown to significantly influence global myocardial slice mean T_1 value, and therefore interfere with the diagnosis of diffuse interstitial fibrosis (6).
6. The hematocrit level will affect the partition coefficient of the gadolinium contrast agent to be considered for the clinical use of T_1 mapping.
7. Even if myocardial T_1 values have been shown to be the same between basal, mid-cavity and apical sections of the LV in healthy volunteers, it is unknown if all sections are affected equally by diffuse interstitial fibrosis. For practical reasons, T_1 maps in patients are performed at a single section level of the LV (usually mid-ventricle). Therefore, this sampling limitation might affect the final T_1 values, in a myocardium where the fibrosis process isn't homogenous.

T_1 mapping is a very sensitive technique that needs to be performed in rigorous conditions in order to enhance its accuracy for fibrosis assessment and allow cross sectional comparisons (75). While postcontrast T_1 value of myocardial fibrosis is significantly different from that of normal myocardium, myocardial T_1 distribution can be significantly scattered and this might limit its sensitivity for disease states with less severe fibrosis.

T_1 mapping is still an emerging technique. Before it can be used for clinical applications, a more standardized histologically validated technique needs to be identified and assessed in clinical studies on various and larger groups of patients and in multicenter settings.

Equilibrium Contrast CMR—Recently Flett et al. reported a new CMR method to assess diffuse myocardial fibrosis: equilibrium contrast CMR (76). This was implemented to improve myocardial T_1 mapping by excluding confounding factors such as heart rate, body composition and renal clearance variability. It is based on 3 elements that are a bolus of gadolinium followed by continuous infusion to achieve blood/myocardium equilibrium, a measurement of the blood volume of distribution (1-hematocrit) and a pre- and postequilibrium T_1 measurement by CMR. This method allows a precise calculation of the gadolinium myocardial volume distribution that reflects diffuse myocardial fibrosis. In a selected population of pre-surgical aortic stenosis and hypertrophic cardiomyopathy patients undergoing myectomy, Flett et al. validated this method against fibrosis quantification by

histology on selective surgical biopsies. They showed that equilibrium contrast CMR correlated strongly with biopsy histological fibrosis. This data is preliminary, and as for T_1 mapping, has to be confirmed in larger and different cardiomyopathy populations. Also this method imposes a more complex image acquisition protocol that questions its clinical applicability at the time when CMR availability is still a major limitation in comparison with other cardiac imaging techniques.

Other Methods to explore Myocardial Fibrosis

This review focuses on CMR as the most promising accessible and accurate noninvasive imaging tool to assess myocardial fibrosis in a routine clinical practice. Other non invasive methods have been used to characterize myocardial fibrosis (perfusable tissue index with positron emission tomography, pro-collagen-derived pro-peptides and matrix metalloproteinases as serum fibrosis biomarkers, single photon emission computed tomography imaging with specific radiolabeled agents) or its functional consequences (tissue doppler echocardiography, CMR tissue tagging) and have been reported in the literature (77) but do not constitute the focus of this review. The cross-sectional combination of different imaging modalities might increase the diagnostic accuracy for myocardial fibrosis, but this still needs to be established.

Future Perspective

CMR has recently been proposed as a comprehensive tool in the clinical arena for the diagnosis and management of patients with heart failure (14). LGE-CMR after showing its prognostic power to predict myocardial recovery in ischemic cardiomyopathy, has also shown its diagnostic accuracy for myocardial replacement fibrosis assessment in different types of cardiomyopathies. LGE presence has a powerful independent clinical prognostic value in ischemic cardiomyopathy (9, 11, 50, 51), but also in all other types of cardiomyopathies (8, 54, 78, 79). This knowledge is now being converted in efficient methods to monitor therapeutic applications through new studies designed to improve our therapeutic options.

The emergence of T_1 mapping further improves our knowledge and the clinical assessment of myocardial diffuse fibrosis and further refines the information provided by LGE-CMR. It might help us to better stratify much larger and lower-cardiovascular risk patient populations (diabetics, hypertensive), detecting subclinical myocardial changes before the onset of diastolic and systolic dysfunction. For the moment, clinical data is scarce and the clinical value of this technique remains to be shown specifically in larger groups of patients and in prospective studies. T_1 mapping using standardized imaging protocols combined with LGE will be of great help for a more precise myocardial tissue characterization. This combination of tissular information might help the clinician to better understand and diagnose sooner the underlying cardiomyopathic process. This information will also help to improve therapeutic strategies and enable a more direct monitoring of their effect, thus improving clinical outcomes (4, 32).

Abbreviations

CMR	cardiovascular magnetic resonance
CVF	collagen volume fraction
LGE	late gadolinium enhancement
SPECT	single photon emission computed tomography
HCM	hypertrophic cardiomyopathy

SCD	sudden cardiac death
LV	left ventricle
MOLLI	Modified look locker inversion recovery

Acknowledgments

Nathan Mewton was supported by a post-doctoral research grant from the French Federation of Cardiology.

This project was also part of a research effort funded by a NIH grant n° P20HL101397 to Dr. Joao AC Lima.

We thank M. Viallon for her advice and assistance on manuscript writing.

References

1. de Leeuw N, Ruiter DJ, Balk AH, de Jonge N, Melchers WJ, Galama JM. Histopathologic findings in explanted heart tissue from patients with end-stage idiopathic dilated cardiomyopathy. Transpl Int. 2001; 14:299–306. [PubMed: 11692213]
2. Marijianowski MM, Teeling P, Mann J, Becker AE. Dilated cardiomyopathy is associated with an increase in the type I/type III collagen ratio: a quantitative assessment. J Am Coll Cardiol. 1995; 25:1263–1272. [PubMed: 7722119]
3. Whittaker P, Boughner DR, Kloner RA. Analysis of healing after myocardial infarction using polarized light microscopy. Am J Pathol. 1989; 134:879–893. [PubMed: 2705508]
4. Diez J, Querejeta R, Lopez B, Gonzalez A, Larman M, Martinez Ubago JL. Losartan-dependent regression of myocardial fibrosis is associated with reduction of left ventricular chamber stiffness in hypertensive patients. Circulation. 2002; 105:2512–2517. [PubMed: 12034658]
5. Conrad CH, Brooks WW, Hayes JA, Sen S, Robinson KG, Bing OH. Myocardial fibrosis and stiffness with hypertrophy and heart failure in the spontaneously hypertensive rat. Circulation. 1995; 91:161–170. [PubMed: 7805198]
6. Iles L, Pfluger H, Phrommintikul A, et al. Evaluation of diffuse myocardial fibrosis in heart failure with cardiac magnetic resonance contrast-enhanced T1 mapping. J Am Coll Cardiol. 2008; 52:1574–1580. [PubMed: 19007595]
7. Schwarz F, Mall G, Zebe H, et al. Quantitative morphologic findings of the myocardium in idiopathic dilated cardiomyopathy. Am J Cardiol. 1983; 51:501–506. [PubMed: 6218745]
8. Assomull RG, Prasad SK, Lyne J, et al. Cardiovascular magnetic resonance, fibrosis, and prognosis in dilated cardiomyopathy. J Am Coll Cardiol. 2006; 48:1977–1985. [PubMed: 17112987]
9. Bello D, Shah DJ, Farah GM, et al. Gadolinium cardiovascular magnetic resonance predicts reversible myocardial dysfunction and remodeling in patients with heart failure undergoing beta-blocker therapy. Circulation. 2003; 108:1945–1953. [PubMed: 14557364]
10. Kwon DH, Halley CM, Popovic ZB, et al. Gender differences in survival in patients with severe left ventricular dysfunction despite similar extent of myocardial scar measured on cardiac magnetic resonance. Eur J Heart Fail. 2009; 11:937–944. [PubMed: 19789396]
11. Kwong RY, Chan AK, Brown KA, et al. Impact of unrecognized myocardial scar detected by cardiac magnetic resonance imaging on event-free survival in patients presenting with signs or symptoms of coronary artery disease. Circulation. 2006; 113:2733–2743. [PubMed: 16754804]
12. Kwong RY, Sattar H, Wu H, et al. Incidence and prognostic implication of unrecognized myocardial scar characterized by cardiac magnetic resonance in diabetic patients without clinical evidence of myocardial infarction. Circulation. 2008; 118:1011–1020. [PubMed: 18725488]
13. Friedrich MG. There is more than shape and function. J Am Coll Cardiol. 2008; 52:1581–1583. [PubMed: 19007596]
14. Karamitsos TD, Francis JM, Myerson S, Selvanayagam JB, Neubauer S. The role of cardiovascular magnetic resonance imaging in heart failure. J Am Coll Cardiol. 2009; 54:1407–1424. [PubMed: 19796734]

15. Mahrholdt H, Wagner A, Judd RM, Sechtem U, Kim RJ. Delayed enhancement cardiovascular magnetic resonance assessment of non-ischaemic cardiomyopathies. Eur Heart J. 2005; 26:1461–1474. [PubMed: 15831557]
16. Karamitsos TD, Hudsmith LE, Selvanayagam JB, Neubauer S, Francis JM. Operator induced variability in left ventricular measurements with cardiovascular magnetic resonance is improved after training. J Cardiovasc Magn Reson. 2007; 9:777–783. [PubMed: 17891615]
17. Mahrholdt H, Wagner A, Holly TA, et al. Reproducibility of chronic infarct size measurement by contrast-enhanced magnetic resonance imaging. Circulation. 2002; 106:2322–2327. [PubMed: 12403661]
18. Pennell DJ, Sechtem UP, Higgins CB, et al. Clinical indications for cardiovascular magnetic resonance (CMR): Consensus Panel report. Eur Heart J. 2004; 25:1940–1965. [PubMed: 15522474]
19. Schaper J, Speiser B. The extracellular matrix in the failing human heart. Basic Res Cardiol. 1992; 87 Suppl 1:303–309. [PubMed: 1497574]
20. Bishop JE, Greenbaum R, Gibson DG, Yacoub M, Laurent GJ. Enhanced deposition of predominantly type I collagen in myocardial disease. J Mol Cell Cardiol. 1990; 22:1157–1165. [PubMed: 2095438]
21. Brooks A, Schinde V, Bateman AC, Gallagher PJ. Interstitial fibrosis in the dilated non-ischaemic myocardium. Heart. 2003; 89(10):1255–1256. [PubMed: 12975439]
22. Roberts WC, Siegel RJ, McManus BM. Idiopathic dilated cardiomyopathy: analysis of 152 necropsy patients. Am J Cardiol. 1987; 60:1340–1355. [PubMed: 3687784]
23. Weber KT, Janicki JS, Shroff SG, Pick R, Chen RM, Bashey RI. Collagen remodeling of the pressure-overloaded, hypertrophied nonhuman primate myocardium. Circ Res. 1988; 62:757–765. [PubMed: 2964945]
24. Boudina S, Abel ED. Diabetic cardiomyopathy revisited. Circulation. 2007; 115:3213–3223. [PubMed: 17592090]
25. Factor SM, Bhan R, Minase T, Wolinsky H, Sonnenblick EH. Hypertensive-diabetic cardiomyopathy in the rat: an experimental model of human disease. Am J Pathol. 1981; 102:219–228. [PubMed: 7468768]
26. Tanaka M, Fujiwara H, Onodera T, Wu DJ, Hamashima Y, Kawai C. Quantitative analysis of myocardial fibrosis in normals, hypertensive hearts, and hypertrophic cardiomyopathy. Br Heart J. 1986; 55:575–581. [PubMed: 3718796]
27. Weber KT, Brilla CG. Pathological hypertrophy and cardiac interstitium. Fibrosis and renin-angiotensin-aldosterone system. Circulation. 1991; 83:1849–1865. [PubMed: 1828192]
28. Schwarz F, Flameng W, Schaper J, et al. Myocardial structure and function in patients with aortic valve disease and their relation to postoperative results. Am J Cardiol. 1978; 41:661–669. [PubMed: 645569]
29. Weidemann F, Herrmann S, Stork S, et al. Impact of myocardial fibrosis in patients with symptomatic severe aortic stenosis. Circulation. 2009; 120:577–584. [PubMed: 19652094]
30. Marijianowski MM, Teeling P, Becker AE. Remodeling after myocardial infarction in humans is not associated with interstitial fibrosis of noninfarcted myocardium. J Am Coll Cardiol. 1997; 30:76–82. [PubMed: 9207624]
31. Martos R, Baugh J, Ledwidge M, et al. Diastolic heart failure: evidence of increased myocardial collagen turnover linked to diastolic dysfunction. Circulation. 2007; 115:888–895. [PubMed: 17283265]
32. Lopez B, Gonzalez A, Beaumont J, Querejeta R, Larman M, Diez J. Identification of a potential cardiac antifibrotic mechanism of torasemide in patients with chronic heart failure. J Am Coll Cardiol. 2007; 50:859–867. [PubMed: 17719472]
33. Lopez B, Querejeta R, Gonzalez A, Sanchez E, Larman M, Diez J. Effects of loop diuretics on myocardial fibrosis and collagen type I turnover in chronic heart failure. J Am Coll Cardiol. 2004; 43:2028–2035. [PubMed: 15172408]
34. Shah KB, Inoue Y, Mehra MR. Amyloidosis and the heart: a comprehensive review. Arch Intern Med. 2006; 166:1805–1813. [PubMed: 17000935]
35. Zarate YA, Hopkin RJ. Fabry's disease. Lancet. 2008; 372:1427–1435. [PubMed: 18940466]

36. Sutton MG, Sharpe N. Left ventricular remodeling after myocardial infarction: pathophysiology and therapy. Circulation. 2000; 101:2981–2988. [PubMed: 10869273]
37. Bohl S, Wassmuth R, Abdel-Aty H, et al. Delayed enhancement cardiac magnetic resonance imaging reveals typical patterns of myocardial injury in patients with various forms of non-ischemic heart disease. Int J Cardiovasc Imaging. 2008; 24:597–607. [PubMed: 18344061]
38. Querejeta R, Lopez B, Gonzalez A, et al. Increased collagen type I synthesis in patients with heart failure of hypertensive origin: relation to myocardial fibrosis. Circulation. 2004; 110:1263–1268. [PubMed: 15313958]
39. Schalla S, Bekkers SC, Dennert R, et al. Replacement and reactive myocardial fibrosis in idiopathic dilated cardiomyopathy: comparison of magnetic resonance imaging with right ventricular biopsy. Eur J Heart Fail. 2010; 12:227–231. [PubMed: 20156939]
40. Croisille P, Revel D, Saeed M. Contrast agents and cardiac MR imaging of myocardial ischemia: from bench to bedside. Eur Radiol. 2006; 16:1951–1963. [PubMed: 16633792]
41. Judd RM, Atalay MK, Rottman GA, Zerhouni EA. Effects of myocardial water exchange on T1 enhancement during bolus administration of MR contrast agents. Magn Reson Med. 1995; 33:215–223. [PubMed: 7707912]
42. Kim RJ, Chen EL, Lima JA, Judd RM. Myocardial Gd-DTPA kinetics determine MRI contrast enhancement and reflect the extent and severity of myocardial injury after acute reperfused infarction. Circulation. 1996; 94:3318–3326. [PubMed: 8989146]
43. Judd RM, Lugo-Olivieri CH, Arai M, et al. Physiological basis of myocardial contrast enhancement in fast magnetic resonance images of 2-day-old reperfused canine infarcts. Circulation. 1995; 92:1902–1910. [PubMed: 7671375]
44. Lima JA, Judd RM, Bazille A, Schulman SP, Atalar E, Zerhouni EA. Regional heterogeneity of human myocardial infarcts demonstrated by contrast-enhanced MRI. Potential mechanisms. Circulation. 1995; 92:1117–1125. [PubMed: 7648655]
45. Kim RJ, Wu E, Rafael A, et al. The use of contrast-enhanced magnetic resonance imaging to identify reversible myocardial dysfunction. N Engl J Med. 2000; 343:1445–1453. [PubMed: 11078769]
46. Kim RJ, Fieno DS, Parrish TB, et al. Relationship of MRI delayed contrast enhancement to irreversible injury, infarct age, and contractile function. Circulation. 1999; 100:1992–2002. [PubMed: 10556226]
47. Ricciardi MJ, Wu E, Davidson CJ, et al. Visualization of discrete microinfarction after percutaneous coronary intervention associated with mild creatine kinase-MB elevation. Circulation. 2001; 103:2780–2783. [PubMed: 11401931]
48. Wu E, Judd RM, Vargas JD, Klocke FJ, Bonow RO, Kim RJ. Visualisation of presence, location, and transmural extent of healed Q-wave and non-Q-wave myocardial infarction. Lancet. 2001; 357:21–28. [PubMed: 11197356]
49. McCrohon JA, Moon JC, Prasad SK, et al. Differentiation of heart failure related to dilated cardiomyopathy and coronary artery disease using gadolinium-enhanced cardiovascular magnetic resonance. Circulation. 2003; 108:54–59. [PubMed: 12821550]
50. Orn S, Manhenke C, Anand IS, et al. Effect of left ventricular scar size, location, and transmurality on left ventricular remodeling with healed myocardial infarction. Am J Cardiol. 2007; 99:1109–1114. [PubMed: 17437737]
51. Bello D, Fieno DS, Kim RJ, et al. Infarct morphology identifies patients with substrate for sustained ventricular tachycardia. J Am Coll Cardiol. 2005; 45:1104–1108. [PubMed: 15808771]
52. Rubinshtein R, Glockner JF, Ommen SR, et al. Characteristics and clinical significance of late gadolinium enhancement by contrast-enhanced magnetic resonance imaging in patients with hypertrophic cardiomyopathy. Circ Heart Fail. 2010; 3:51–58. [PubMed: 19850699]
53. Kwon DH, Smedira NG, Rodriguez ER, et al. Cardiac magnetic resonance detection of myocardial scarring in hypertrophic cardiomyopathy: correlation with histopathology and prevalence of ventricular tachycardia. J Am Coll Cardiol. 2009; 54:242–249. [PubMed: 19589437]
54. Austin BA, Tang WH, Rodriguez ER, et al. Delayed hyper-enhancement magnetic resonance imaging provides incremental diagnostic and prognostic utility in suspected cardiac amyloidosis. JACC Cardiovasc Imaging. 2009; 2:1369–1377. [PubMed: 20083070]

55. Azevedo CF, Nigri M, Higuchi ML, et al. Prognostic Significance of Myocardial Fibrosis Quantification by Histopathology and Magnetic Resonance Imaging in Patients With Severe Aortic Valve Disease. J Am Coll Cardiol. 2010; 56:278–287. [PubMed: 20633819]
56. Krittayaphong R, Boonyasirinant T, Chaithiraphan V, et al. Prognostic value of late gadolinium enhancement in hypertensive patients with known or suspected coronary artery disease. Int J Cardiovasc Imaging. 2010; 26 Suppl 1:123–131. [PubMed: 20049536]
57. Hendel RC, Patel MR, Kramer CM, et al. ACCF/ACR/SCCT/SCMR/ASNC/NASCI/SCAI/SIR 2006 appropriateness criteria for cardiac computed tomography and cardiac magnetic resonance imaging: a report of the American College of Cardiology Foundation Quality Strategic Directions Committee Appropriateness Criteria Working Group, American College of Radiology, Society of Cardiovascular Computed Tomography, Society for Cardiovascular Magnetic Resonance, American Society of Nuclear Cardiology, North American Society for Cardiac Imaging, Society for Cardiovascular Angiography and Interventions, and Society of Interventional Radiology. J Am Coll Cardiol. 2006; 48:1475–1497. [PubMed: 17010819]
58. Simonetti OP, Kim RJ, Fieno DS, et al. An improved MR imaging technique for the visualization of myocardial infarction. Radiology. 2001; 218:215–223. [PubMed: 11152805]
59. Spiewak M, Malek LA, Misko J, et al. Comparison of different quantification methods of late gadolinium enhancement in patients with hypertrophic cardiomyopathy. Eur J Radiol. 2009
60. Amado LC, Gerber BL, Gupta SN, et al. Accurate and objective infarct sizing by contrast-enhanced magnetic resonance imaging in a canine myocardial infarction model. J Am Coll Cardiol. 2004; 44:2383–2389. [PubMed: 15607402]
61. Bondarenko O, Beek AM, Hofman MB, et al. Standardizing the definition of hyperenhancement in the quantitative assessment of infarct size and myocardial viability using delayed contrast-enhanced CMR. J Cardiovasc Magn Reson. 2005; 7:481–485. [PubMed: 15881532]
62. Hsu LY, Ingkanisorn WP, Kellman P, Aletras AH, Arai AE. Quantitative myocardial infarction on delayed enhancement MRI. Part II: Clinical application of an automated feature analysis and combined thresholding infarct sizing algorithm. J Magn Reson Imaging. 2006; 23:309–314. [PubMed: 16450368]
63. Yan AT, Shayne AJ, Brown KA, et al. Characterization of the peri-infarct zone by contrast-enhanced cardiac magnetic resonance imaging is a powerful predictor of post-myocardial infarction mortality. Circulation. 2006; 114:32–39. [PubMed: 16801462]
64. Schmidt A, Azevedo CF, Cheng A, et al. Infarct tissue heterogeneity by magnetic resonance imaging identifies enhanced cardiac arrhythmia susceptibility in patients with left ventricular dysfunction. Circulation. 2007; 115:2006–2014. [PubMed: 17389270]
65. Messroghli DR, Radjenovic A, Kozerke S, Higgins DM, Sivananthan MU, Ridgway JP. Modified Look-Locker inversion recovery (MOLLI) for high-resolution T1 mapping of the heart. Magn Reson Med. 2004; 52:141–146. [PubMed: 15236377]
66. Maceira AM, Joshi J, Prasad SK, et al. Cardiovascular magnetic resonance in cardiac amyloidosis. Circulation. 2005; 111:186–193. [PubMed: 15630027]
67. Messroghli DR, Greiser A, Frohlich M, Dietz R, Schulz-Menger J. Optimization and validation of a fully-integrated pulse sequence for modified look-locker inversion-recovery (MOLLI) T1 mapping of the heart. J Magn Reson Imaging. 2007; 26:1081–1086. [PubMed: 17896383]
68. Flacke SJ, Fischer SE, Lorenz CH. Measurement of the gadopentetate dimeglumine partition coefficient in human myocardium in vivo: normal distribution and elevation in acute and chronic infarction. Radiology. 2001; 218:703–710. [PubMed: 11230643]
69. Messroghli DR, Niendorf T, Schulz-Menger J, Dietz R, Friedrich MG. T1 mapping in patients with acute myocardial infarction. J Cardiovasc Magn Reson. 2003; 5:353–359. [PubMed: 12765114]
70. Messroghli DR, Plein S, Higgins DM, et al. Human myocardium: single-breath-hold MR T1 mapping with high spatial resolution--reproducibility study. Radiology. 2006; 238:1004–1012. [PubMed: 16424239]
71. Messroghli DR, Walters K, Plein S, et al. Myocardial T1 mapping: application to patients with acute and chronic myocardial infarction. Magn Reson Med. 2007; 58:34–40. [PubMed: 17659622]

72. Kehr E, Sono M, Chugh SS, Jerosch-Herold M. Gadolinium-enhanced magnetic resonance imaging for detection and quantification of fibrosis in human myocardium in vitro. Int J Cardiovasc Imaging. 2008; 24:61–68. [PubMed: 17429755]

73. Slavin, GS.; Song, T.; Stainsby, JA. The effect of heart rate in Look-Locker Cardiac T1 mapping. International Society for Magnetic Resonance in Medicine 19th Annual Scientific Meeting; International Society for Magnetic Resonance in Medicine 19th Annual Scientific Meeting; 2010.

74. Song, T.; Ho, VB.; Slavin, G.; Hood, MN.; Stainsby, JA. Clinical evaluation of a cardiac T1 mapping method using a reduced number of sample times. International Society for Magnetic Resonance in Medicine 19th Annual Scientific Meeting; International Society for Magnetic Resonance in Medicine 19th Annual Scientific Meeting; 2010. Abstract 5017

75. Gai N, Turkbey EB, Nazarian S, et al. T1 Mapping of the Gadolinium–enhanced Myocardium: Adjustment for Factors Affecting Inter-patient Comparison. Magn Reson Med. In Press.

76. Flett AS, Hayward MP, Ashworth MT, et al. Equilibrium contrast cardiovascular magnetic resonance for the measurement of diffuse myocardial fibrosis: preliminary validation in humans. Circulation. 2010; 122:138–144. [PubMed: 20585010]

77. Jellis C, Martin J, Narula J, Marwick TH. Assessment of nonischemic myocardial fibrosis. J Am Coll Cardiol. 2010; 56:89–97. [PubMed: 20620723]

78. Bogun FM, Desjardins B, Good E, et al. Delayed-enhanced magnetic resonance imaging in nonischemic cardiomyopathy: utility for identifying the ventricular arrhythmia substrate. J Am Coll Cardiol. 2009; 53:1138–1145. [PubMed: 19324259]

79. Nigri M, Azevedo CF, Rochitte CE, et al. Contrast-enhanced magnetic resonance imaging identifies focal regions of intramyocardial fibrosis in patients with severe aortic valve disease: Correlation with quantitative histopathology. Am Heart J. 2009; 157:361–368. [PubMed: 19185646]

80. Konduracka E, Gackowski A, Rostoff P, Galicka-Latala D, Frasik W, Piwowarska W. Diabetes-specific cardiomyopathy in type 1 diabetes mellitus: no evidence for its occurrence in the era of intensive insulin therapy. Eur Heart J. 2007; 28:2465–2471. [PubMed: 17766928]

81. Moreo A, Ambrosio G, De Chiara B, et al. Influence of myocardial fibrosis on left ventricular diastolic function: noninvasive assessment by cardiac magnetic resonance and echo. Circ Cardiovasc Imaging. 2009; 2:437–443. [PubMed: 19920041]

82. Nanjo S, Yoshikawa K, Harada M, et al. Correlation between left ventricular diastolic function and ejection fraction in dilated cardiomyopathy using magnetic resonance imaging with late gadolinium enhancement. Circ J. 2009; 73:1939–1944. [PubMed: 19729860]

83. Nazarian S, Bluemke DA, Lardo AC, et al. Magnetic resonance assessment of the substrate for inducible ventricular tachycardia in nonischemic cardiomyopathy. Circulation. 2005; 112:2821–2825. [PubMed: 16267255]

84. Soriano CJ, Ridocci F, Estornell J, Jimenez J, Martinez V, De Velasco JA. Noninvasive diagnosis of coronary artery disease in patients with heart failure and systolic dysfunction of uncertain etiology, using late gadolinium-enhanced cardiovascular magnetic resonance. J Am Coll Cardiol. 2005; 45:743–748. [PubMed: 15734620]

85. Wu KC, Weiss RG, Thiemann DR, et al. Late gadolinium enhancement by cardiovascular magnetic resonance heralds an adverse prognosis in nonischemic cardiomyopathy. J Am Coll Cardiol. 2008; 51:2414–2421. [PubMed: 18565399]

86. Aquaro GD, Masci P, Formisano F, et al. Usefulness of delayed enhancement by magnetic resonance imaging in hypertrophic cardiomyopathy as a marker of disease and its severity. Am J Cardiol. 2010; 105:392–397. [PubMed: 20102955]

87. Boonyasirinant T, Rajiah P, Setser RM, et al. Aortic stiffness is increased in hypertrophic cardiomyopathy with myocardial fibrosis: novel insights in vascular function from magnetic resonance imaging. J Am Coll Cardiol. 2009; 54:255–262. [PubMed: 19589439]

88. Choudhury L, Mahrholdt H, Wagner A, et al. Myocardial scarring in asymptomatic or mildly symptomatic patients with hypertrophic cardiomyopathy. J Am Coll Cardiol. 2002; 40:2156–2164. [PubMed: 12505229]

89. Debl K, Djavidani B, Buchner S, et al. Delayed hyperenhancement in magnetic resonance imaging of left ventricular hypertrophy caused by aortic stenosis and hypertrophic cardiomyopathy: visualisation of focal fibrosis. Heart. 2006; 92:1447–1451. [PubMed: 16606864]
90. Doesch C, Huck S, Bohm CK, et al. Visual estimation of the extent of myocardial hyperenhancement on late gadolinium-enhanced CMR in patients with hypertrophic cardiomyopathy. Magn Reson Imaging. 2010
91. Maron MS, Maron BJ, Harrigan C, et al. Hypertrophic cardiomyopathy phenotype revisited after 50 years with cardiovascular magnetic resonance. J Am Coll Cardiol. 2009; 54:220–228. [PubMed: 19589434]
92. Moon JC, McKenna WJ, McCrohon JA, Elliott PM, Smith GC, Pennell DJ. Toward clinical risk assessment in hypertrophic cardiomyopathy with gadolinium cardiovascular magnetic resonance. J Am Coll Cardiol. 2003; 41:1561–1567. [PubMed: 12742298]
93. Rudolph A, Abdel-Aty H, Bohl S, et al. Noninvasive detection of fibrosis applying contrast-enhanced cardiac magnetic resonance in different forms of left ventricular hypertrophy relation to remodeling. J Am Coll Cardiol. 2009; 53:284–291. [PubMed: 19147047]
94. Schulz-Menger J, Abdel-Aty H, Rudolph A, et al. Gender-specific differences in left ventricular remodelling and fibrosis in hypertrophic cardiomyopathy: insights from cardiovascular magnetic resonance. Eur J Heart Fail. 2008; 10:850–854. [PubMed: 18692438]
95. Bruder O, Wagner A, Jensen CJ, et al. Myocardial scar vizualized by CMR Imaging predicts major adverse events in patients with hypertrophic cardiomyopathy. In Press.
96. O'Hanlon RM, Grasso A, Roughton M, et al. Pronostic Significance of Myocardial Fibrosis in Hypertrophic Cardiomyopathy. In Press.
97. Nassenstein K, Bruder O, Breuckmann F, Erbel R, Barkhausen J, Schlosser T. Prevalence, pattern, and functional impact of late gadolinium enhancement in left ventricular hypertrophy due to aortic valve stenosis. Rofo. 2009; 181:472–476. [PubMed: 19241322]
98. Cheong BY, Muthupillai R, Nemeth M, et al. The utility of delayed-enhancement magnetic resonance imaging for identifying nonischemic myocardial fibrosis in asymptomatic patients with biopsy-proven systemic sarcoidosis. Sarcoidosis Vasc Diffuse Lung Dis. 2009; 26:39–46. [PubMed: 19960787]
99. Patel MR, Cawley PJ, Heitner JF, et al. Detection of myocardial damage in patients with sarcoidosis. Circulation. 2009; 120:1969–1977. [PubMed: 19884472]
100. Smedema JP, Snoep G, van Kroonenburgh MP, et al. Evaluation of the accuracy of gadolinium-enhanced cardiovascular magnetic resonance in the diagnosis of cardiac sarcoidosis. J Am Coll Cardiol. 2005; 45:1683–1690. [PubMed: 15893188]
101. Steen H, Merten C, Refle S, et al. Prevalence of different gadolinium enhancement patterns in patients after heart transplantation. J Am Coll Cardiol. 2008; 52:1160–1167. [PubMed: 18804744]
102. Pepe A, Positano V, Capra M, et al. Myocardial scarring by delayed enhancement cardiovascular magnetic resonance in thalassaemia major. Heart. 2009; 95:1688–1693. [PubMed: 19491092]
103. Rochitte CE, Oliveira PF, Andrade JM, et al. Myocardial delayed enhancement by magnetic resonance imaging in patients with Chagas' disease: a marker of disease severity. J Am Coll Cardiol. 2005; 46:1553–1558. [PubMed: 16226184]
104. Schietinger BJ, Brammer GM, Wang H, et al. Patterns of late gadolinium enhancement in chronic hemodialysis patients. JACC Cardiovasc Imaging. 2008; 1:450–456. [PubMed: 19356466]
105. Sparrow P, Messroghli DR, Reid S, Ridgway JP, Bainbridge G, Sivananthan MU. Myocardial T1 mapping for detection of left ventricular myocardial fibrosis in chronic aortic regurgitation: pilot study. AJR Am J Roentgenol. 2006; 187:W630–W635. [PubMed: 17114517]

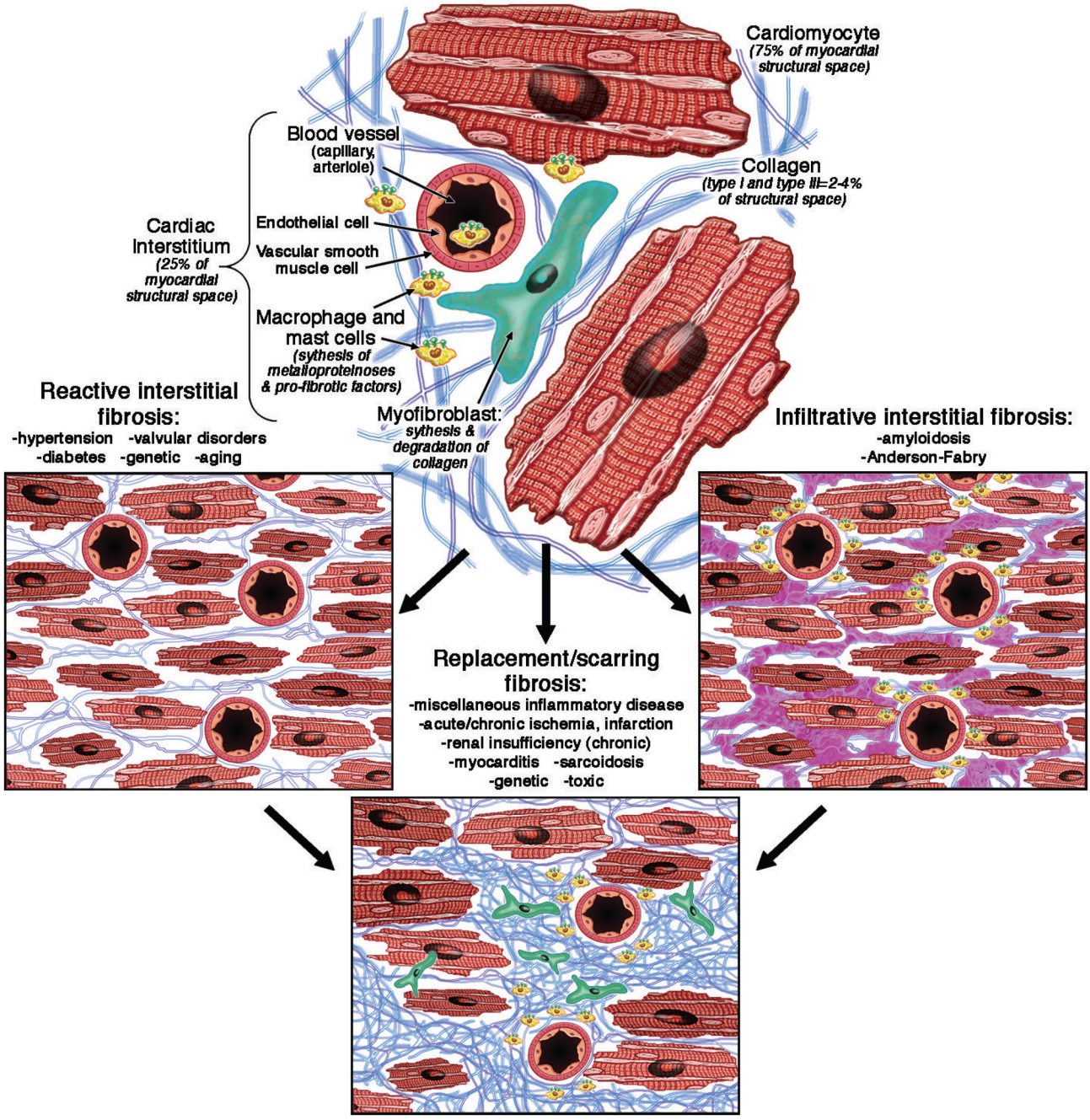

Figure 1.

Etiophysiopathology of Myocardial Fibrosis. Myocardial fibrosis is a complex process that involves each cellular component of the myocardial tissue. The myocardial fibroblast has a central position in this process by increasing the production of collagen and other extracellular matrix components under the influence of various factors (renin-angiotensin system, myocyte apoptosis, pro-inflammatory cytokines, reactive oxygen species).

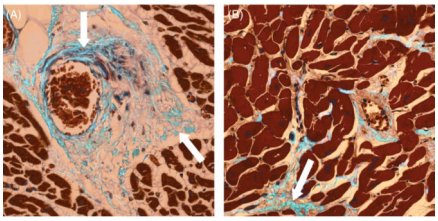

Figure 2.

Diabetic cardiomyopathy: mild myocardial interstitial fibrosis stained in blue with Masson trichrome (white arrow) in a patient with long-duration type 1 diabetes mellitus at autopsy, with perivascular fibrosis (A) and mild fibrosis between myocytes (B). Reprinted with permission Konduracka et al. (80)

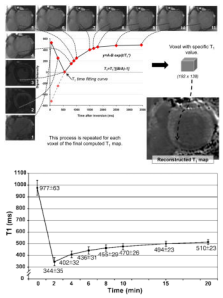

Figure 3.

A) T_1 map Construction. T_1 map after 15 minutes of gadolinium administration in a inferior infarct case. This is the modified look-locker inversion recovery sequence that uses 17 heart-beats to reconstruct 11 images with different inversion times during mid-diastole. It is necessary to combine all images to generate the final T1 map. For that, it is necessary to apply algorithms to define the best fitting curve over the 11 acquired initial voxels linking for the same location. Those fitting algorithm are very sensitive to motion and image quality/artifacts. The result is a T1 map imaging where the T1 time for the global or segmented LV can be assessed.

B) T_1 Recovery Graph after Contrast Administration. Graph showing the recovery of absolute myocardial T_1 value in a healthy heart (short-axis, mid-ventricle) at different time points prior and after contrast administration (0, 2, 4, 6, 8, 10, 15 and 20 minutes). T_1 values are expressed as means ± standard deviations. The global and regional mean T_1 values will vary significantly significantly with the time of assessment. The standard deviation of T_1 value is more significant prior to contrast administration. Reprinted with permission, from Messroghli et al. (70)

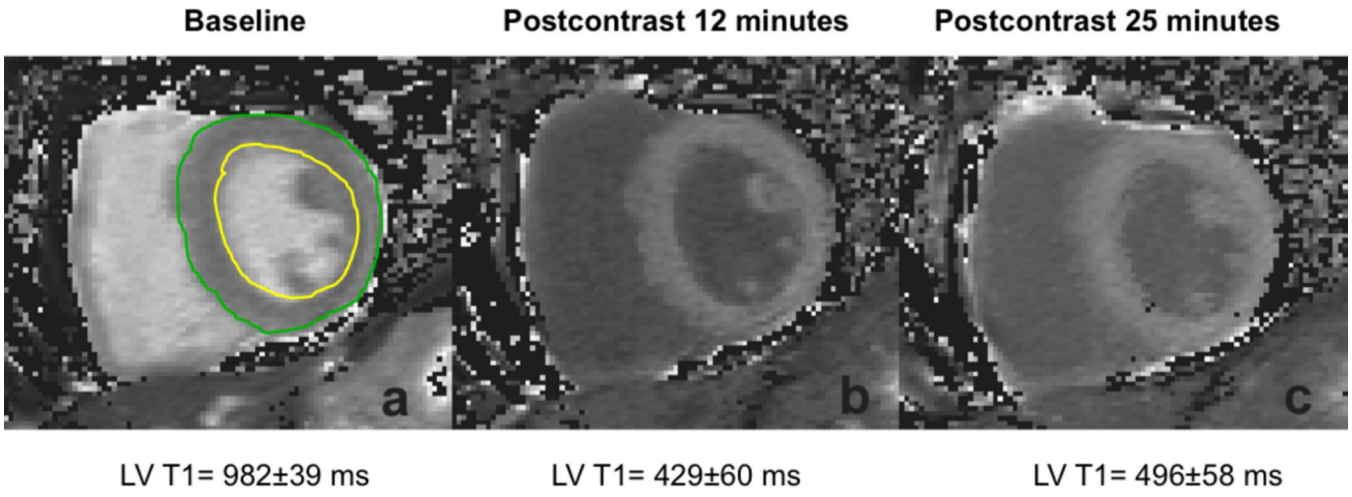

Figure 4.

T_1 maps of the myocardium at the mid-ventricular short axis level in a healthy volunteer, a) Pre-contrast, b) post gadolinium contrast (0.15 mmol/kg) at 12 minutes c) and 25 minutes acquired with the MOLLI sequence. The mean T_1 value for the left ventricle (LV) can be obtained at each time after tracing the endocardial and epicardial countours of the LV (a).

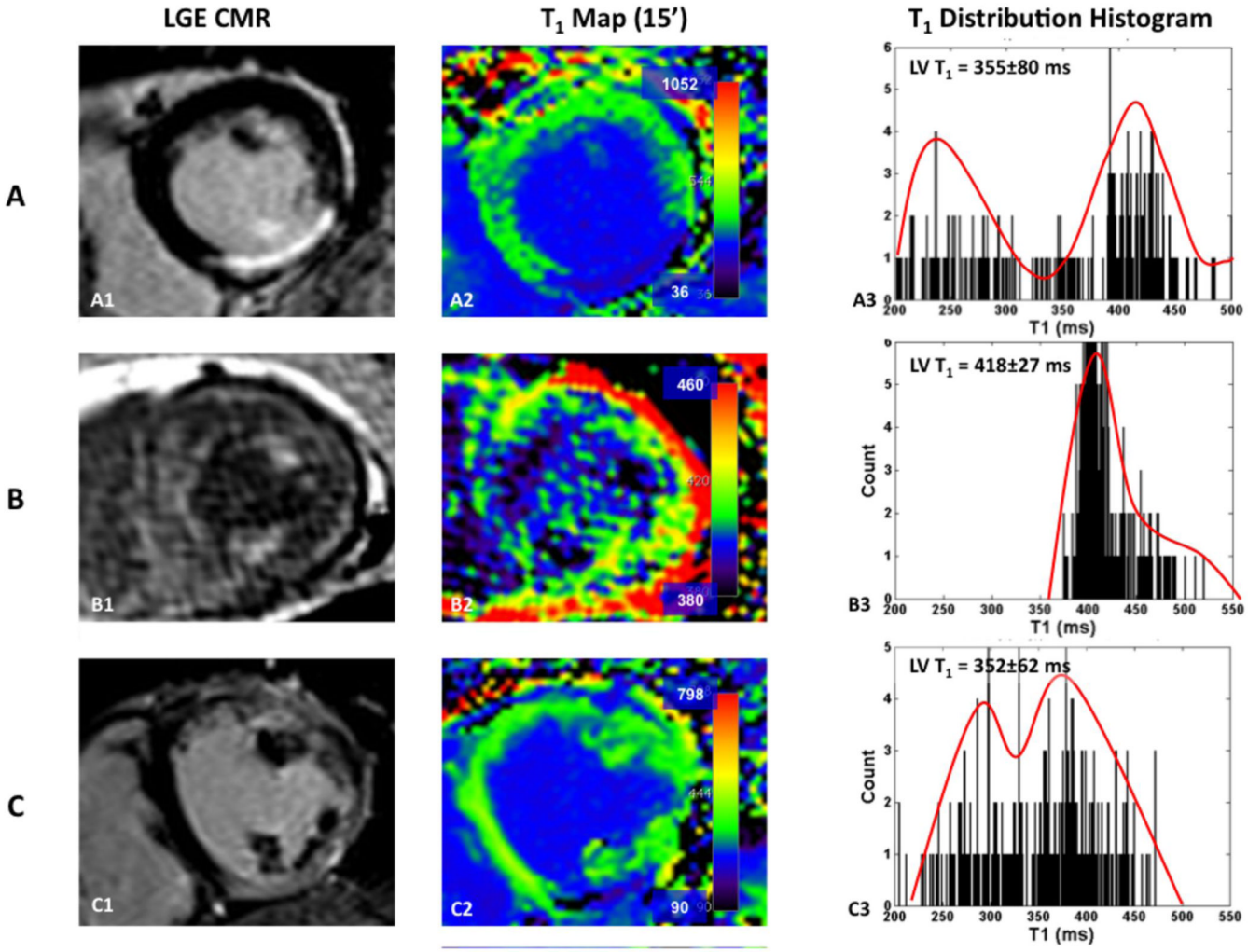

Figure 5.

Comparison of late gadolinium enhanced studies with corresponding T_1 maps and T_1 values distribution histograms in different cardiomyopathies: A) Chronic inferior myocardial infarction; B) Cardiac amyloïdosis; C) Non Ischemic Dilated Cardiomyopathy. In each example, the short axis late gadolinium images shows images with different patterns of enhancement, transmural localized in the case of a myocardial infarction scar (A1), sub-endocardial diffuse in the case of cardiac amyloïdosis (B1) or sub-epicardial and heterogeneous in the case of dilated cardiomyopathy. In the middle panel are the corresponding T_1 maps (A2, B2, B3) obtained after MOLLI acquisitions. From those T_1 maps, a mean left ventricular (LV) T_1 value can be obtained. This information can also be processed more precisely through the analysis of the distribution histogram of the LV T_1 values. Very distinct patterns of distributions can be seen on those examples, but this has to be shown in further larger clinical studies. This might also be a new way to assess and quantify myocardial fibrosis.

Table 1

Different Prevalence reports of myocardial scarring/fibrosis of the left ventricle in various non-ischemic cardiac pathologies as defined with Qualitative Analysis of Late Gadolinium Enhanced CMR.

Cardiac Disease Category	Total number of patient (n)	Prevalence of fibrosis (%)	Range of prevalence (%)	LGE pattern	LGE preferential location
NIDCM (8, 39, 49, 81–85)	350	47	[9; 88]	midwall, patchy foci, subendocardial non-systemised	septum, RV-LV insertion points
HCM (52, 53, 81, 86–96)	1654	69	[45; 100]	midwall, diffuse, heterogeneous	within hypertrophied regions, RV-LV insertion points
Aortic Valve Disease (79, 93, 97)	153	46	[27; 62]	midwall, multifocal	very variable, basal septum and inferior walls
Pulmonary Sarcoidosis (98–100)	170	28	[26; 32]	midwall, subepicardial, ischemic-like	inferoseptal-, inferolateral-basal
Cardiac Amyloidosis (54, 66)	54	72.5	[69; 76]	diffuse subendocardial, patchy subendocardial	global
Hypertensive Cardiomyopathy (56, 93)	1670	39	[28; 50]	patchy, non-specific, Ischemic pattern	none
Diabetic Cardiomyopathy (12)	107	28	NA	non-specific, ischemic pattern	none
Heart Transplant (101)	53	51	NA	ischemic pattern, midwall, diffuse, spotted	Infero-septal
Thalassemia Major (102)	115	24	NA	multifocal, epicardial, midwall	Infero-septal, septum
Chagas' Disease (103)	51	69	NA	subendocardial ischemic –like, subepicardial	Infero-lateral, global
Chronic Hemodialysis (104)	24	79	NA	ischemic pattern, diffuse, midwall-focal	none

NIDCM=non ischemic dilated cardiomyopathy; HCM= hypertrophied cardiomyopathy; LGE=late gadolinium enhancement, LV= left ventricle, RV=right ventricle..

Table 2

Clinical Studies Using T_1 Mapping

Authors	Cardiac Disease Category	Patient Sample Size (n)	T_1 Mapping Method	Results
Messroghli et al. (69)	Acute Myocardial Infarction	8	NA	• T_1 precontrast value of the infarcted myocardium was significantly prolonged (+18±7%) compared to non infarcted normal myocardium. • T_1 10' postcontrast value of the infarct was significantly reduced (−27±4%) compared to normal myocardium
Messroghli et al. (71)	Chronic Myocardial Infarction	24	MOLLI	• T_1 precontrast value of the infarcted myocardium was significantly prolonged compared to non infarcted normal myocardium (1060±61 ms vs. 987±34 ms). • T_1 postcontrast value of the infarct was significantly reduced compared to normal myocardium. • Difference between baseline and postcontrast T_1s significantly more pronounced in the acute than in the chronic studies at all time points.
Sparrow et al. (105)	Chronic Aortic Regurgitation	8	MOLLI	• No significant difference in slice averaged myocardial T_1 pre- and postcontrast values in the patient group compared with controls.
Maceira et al. (66)	Cardiac Amyloidosis	22	NA	• Subendocardial T_1 postcontrast value at 4 minutes was significantly shorter in amyloid patients than in controls (427±73 ms vs. 579±75 ms).
Iles et al. (6)	Chronic Heart Failure	25	VAST	• T_1 15' postcontrast values correlated significantly with collagen volume fraction on myocardial biopsies (R= −0.7). T_1 15' postcontrast values were significantly shorter in heart failure patients than controls (383±17 ms vs 564±23 ms) even after exclusion of LGE areas.